Circular Dichroism Microscopy of Compact Forms of DNA and Chromatin in Vivo and in Vitro: Cholesteric Liquid-Crystalline Phases of DNA and Single Dinoflagellate Nuclei†

Françoise Livolant‡ and Marcos F. Maestre*

Centre de Biologie Cellulaire, CNRS, 67 rue Maurice Günsbourg, 94200 Ivry-sur-Seine, France, and Lawrence Berkeley Laboratory, 1 Cyclotron Road, Berkeley, California 94720

Received July 17, 1987; Revised Manuscript Received December 18, 1987

ABSTRACT: Two highly condensed structures of DNA have been analyzed in the circular dichroism (CD) microscope: the cholesteric liquid-crystalline phase of DNA and the nucleus of a dinoflagellate (*Prorocentrum micans*). In both cases, the DNA shows a helical cholesteric organization, but the helical pitch equals about 2500 nm in the first case and 250 nm in the second one. Since the absorption band of DNA is located at 260 nm, the reflection and absorption bands are well separated in the cholesteric phase of DNA and are overlapping in the dinoflagellate nucleus. However, both structures give a very strong negative CD signal at 265 nm. We show that this very strong signal cannot correspond to a Borrmann effect, i.e., to a superposition of the absorption and reflection bands, but is a differential absorption of left versus right circularly polarized light. This anomalous differential absorption is probably due to a significant scattering of light, inside of the structure, which produces a resonance phenomenon in the absorption band of the chromophore. Therefore, for any helical structure containing a chromophore, the apparent CD can be expressed as

$$CD = [(\epsilon_L - \epsilon_R)cl] + (\psi_L - \psi_R) + (s_L - s_R)$$

The first term is true absorption and is located in the absorption band of the chromophore, and the last term is true scattering and is observed at the wavelength corresponding to the helical pitch of the structure. The second term $(\psi_L - \psi_R)$ corresponds to the anomalous differential absorption observed in dense superhelical structures of DNA. It superimposes to the first term in the absorption band of the chromophore. $\psi_L - \psi_R$ is a measure of the perfection of the helical structure and of the density of chromophores in the material. Intercalative dyes [ethidium bromide and *meso*-tetrakis(4-*N*-methylpyridyl)porphine (H_2TMpyP-4) and its nickel(II) derivative (Ni^{II}TMpyP-4)] were inserted in the dinoflagellate chromatin. The CD signal recorded in their absorption band mimics the signal observed in the absorption band of DNA. In both structures, the negative sign of the CD at 265 nm indicates that the twist occurring between DNA molecules is left-handed, and we show that this situation is the most frequently encountered in vivo and in vitro.

The optical properties of the condensed forms of DNA have been most often studied in suspensions. The condensation of DNA can be induced by a large variety of ways, i.e., by polymers and salts (Jordan et al., 1972; Laemmli, 1975; Evdokimov et al., 1976), H1 or H5 histones (Adler & Fasman, 1971; Sponar & Fric, 1972), polylysine (Haynes et al., 1970), polyhistidine (Burchardt et al., 1973), divalent metallic ions (Simpson & Sober, 1970; Shin & Eichhorn, 1977), or lithium (Wolf et al., 1977) or simply by dehydration (Tunis-Schneider & Maestre, 1970; Brunner & Maestre, 1974) or in alcoholic solution (Reich et al., 1980; Huey & Mohr, 1981). All these techniques produce a *local* dense packing of DNA in the form of microscopic aggregates. The optical properties of these aggregates are usually studied in suspension and give very strong circular dichroism (CD) signals, either positive or negative, which have been interpreted as the effet of the higher order organization of the DNA molecules in these aggregates (Tunis-Schneider & Maestre, 1970; Lerman, 1971; Jordan et al., 1972). This was confirmed when Maniatis et al. (1974) demonstrated that the secondary structure of DNA is still in the B form in these aggregates. Therefore, alteration of secondary structure was not the cause of the large CD signals.

We will consider here the optical properties of highly condensed forms of DNA which present a *long-range* order instead of a local packing, and two materials will be considered: cholesteric liquid-crystalline phases of DNA and the dinoflagellate nuclei.

DNA has been shown to form liquid-crystalline phases in concentrated aqueous solution (Robinson, 1961, 1966; Lerman, 1973; Livolant, 1984a, 1986, 1987; Livolant & Bouligand, 1986; Rill, 1986), and different phases have been described depending on the DNA concentration (Livolant, 1986, 1987; Livolant & Bouligand, 1986). Liquid crystals represent a special state of the matter which is intermediate between the perfectly ordered structure of the crystal and the total disorder of the amorphous state. Indeed, in a liquid crystal, molecules are able to move with respect to each other, but they must follow certain constraints of orientation. In a cholesteric liquid crystal, molecules present a regular twist of their orientation, giving rise to a helical structure in which molecules are all normal to the helical axis. This liquid-crystalline state reveals the existence of self-organization properties of the DNA molecules themselves in vitro. But a similar organization of DNA has also been described in vivo in special kinds of chromosomes, namely, the dinoflagellate chromosomes (Bouligand et al., 1968; Livolant & Bouligand, 1978), certain

† This research was supported by grants from the National Institutes of Health (AI 08427) and U.S. Department of Energy (DE-AC03-76SF00098).

* Address correspondence to this author at the Lawrence Berkeley Laboratory.

‡ Centre de Biologie Cellulaire, CNRS.

0006-2960/88/0427-3056$01.50/0

bacterial nucleoids (Gourret, 1978), and the DNA of special kinds of mitochondria (Brugerolles & Mignot, 1979). This cholesteric organization is mainly characterized by special patterns when thin sections of these materials are observed in the electron microscope, i.e., series of nested arcs which have been interpreted as the visualization, in projection onto an oblique section plane, of the helical organization of the nucleofilaments (Bouligand et al., 1968). We chose to study one example of these in vivo condensed forms of DNA: the nuclei of the dinoflagellate *Prorocentrum micans* since it is the species that possesses some of the largest known chromosomes and whose geometry is well-known (Bouligand et al., 1968; Livolant & Bouligand, 1978). The nucleus of *P. micans* is very large, with an average volume of 3450 μm^3 corresponding to an estimated DNA content of 7.0×10^{10} nucleotides pairs (Haapala & Soyer, 1973). Dinoflagellates are primitive eukaryotes, and in their nucleus, always enclosed by the nuclear envelope, most of the chromatin is condensed throughout the whole cell cycle into chromosomes. A small part of the chromatin is transcriptionally active and dispersed in the nucleoplasm (Babillot, 1970). This decondensed chromatin corresponds to extrachromosomal loops which are going out and back to the chromosomal body. Whatever the dinoflagellate species, the chemical composition of the chromatin seems to be in the same range with the average ratios of RNA/DNA, acid proteins/DNA, basic proteins/DNA, and total proteins/DNA of 0.39, 0.63, 0.13, and 0.76, respectively (Rizzo et al., 1982). This chromatin is therefore characterized by a very low proportion of basic proteins, among which two proteins of M_r 12 000 and 13 000 have been characterized in *P. micans* (Herzog & Soyer, 1981). Moreover, this chromatin does not show the nucleosomic structure described in eukaryotes (Livolant & Bouligand, 1980; Rizzo & Burghardt, 1980; Herzog & Soyer, 1981). The DNA composition of the dinoflagellate DNA also presents some peculiarities since an atypical base, 5-(hydroxymethyl)uracil, replaces about 40% of the thymines in some species (Rae, 1973; Rae & Steale, 1978) and 62.8% in *P. micans* (Herzog et al., 1982).

The dinoflagellate chromosomes are elongated rods, and the cholesteric axis of the structure is parallel to the elongation axis of the chromosome. This indicates that the DNA molecule is also always normal to the axis of the chromosome. The half-helical pitch, measured on longitudinal sections of the chromosomes, can vary from 800 to 2000 Å, with an average value of 1240 Å (Livolant & Bouligand, 1978). The geometry of these chromosomes is described in the Appendix (Figure A1).

We will therefore consider these two forms of highly condensed DNA either completely pure (the in vitro cholesteric phase of DNA) or associated with proteins and RNA (the dinoflagellate chromatin). However, the geometry of these two structures is similar (helical structure with molecules normal to the helical axis), and this is an important point since examples of a well-known organization of DNA is chromosomes are very rare.

Moreover, these two materials provide the opportunity to study two structures showing the same geometry but with two different relative positions of wavelength of absorption and reflection bands. It has been found that a selective reflection of circularly reflected light occurs in cholesteric structures in the wavelength range corresponding to the helical periodicity of the structure (de Vries, 1951; Robinson, 1966). The two materials studied here present different helical pitches [2500 nm for the cholesteric phases of DNA as measured in the analyzed preparations and about 250 nm for the *P. micans* chromosomes (Livolant & Bouligand, 1978)]. Therefore, $\lambda_{absorption}$ (λ_{abs}) and $\lambda_{reflection}$ (λ_0) are completely separated in the first case (λ_{abs} = 260 nm and λ_0 = 2500 nm) whereas they are overlapping in the second material (λ_{abs} = 260 nm and λ_0 = 250 nm). It is significant that Nitayanada et al. (1973) and Suresh (1976) have shown that in cholesteric liquid crystals a phenomenon of anomalous transmission occurs when absorption bands of chromophores are located close to the reflection band of the structure [Borrmann effect for liquid crystals, Chandrasekhar (1977)].

In this work some dyes were also inserted in the dinoflagellate chromosomes. It is well-known that chromophores that are present in a cholesteric structure show in their absorption band a CD signal that mimics the signal observed in the reflection band of the structure (Saeva, 1979). The chromophore can be either the molecule constituting the cholesteric phase itself or a molecule inserted in the structure. This phenomenon was described as the liquid crystal induced circular dichroism (LCICD), and the sign of the CD signal itself can be either of the same sign or reversed and is controlled by a large number of factors (Saeva et al., 1973). Most recently, Evdokimov et al. (1985) and Phillips et al. (1986) showed in the same way that the insertion of dyes in polymer- and salt-induced (Ψ) DNA aggregates was a good tool to analyze the organization of the DNA itself. By looking at the CD signal of the Ψ-type DNA, in the wavelength range of the dye it was possible to get a signal that mimics the signal obtained in the absorption band of the DNA itself, or which is reversed according as the transition dipole of the inserted dye is either mostly perpendicular or parallel to the axis of the molecule.

Therefore, selected areas of the cholesteric phase showing a precise orientation of the cholesteric axis have been chosen, as well as individual *P. micans* nuclei, and their optical CD properties have been studied by the use of a CD microscope previously described by Maestre and Katz (1982). This device was shown to be specially useful in the study of individual nuclei (Maestre et al., 1985). We report here the existence of very strong CD signals in the dinoflagellate chromosomes (several times the amplitude of the Ψ-type CD signal of the DNA aggregates). The signals obtained with the cholesteric liquid-crystalline phases of DNA are again of a higher order of magnitude. We will show that these enormous signals are related to the long-range chiral organization of DNA in these structures.

Materials and Methods

Chemicals. Ethidium bromide (E8751) was purchased from Sigma; a 0.1 mM stock solution was prepared in 10 mM tris(hydroxymethyl)aminomethane hydrochloride (Tris-HCl), pH 7.4, and stored at 4 °C. Bisbenzimide (Hoechst 33342), M_r 561.9, was purchased from Calbiochem (lot no. 505023), and a 0.1 mM stock solution was prepared in 10 mM Tris-HCl, pH 7.4. Unsubstituted *meso*-tetrakis(4-*N*-methylpyridyl)porphine (H_2TMPyP-4) and its nickel(II) derivative (Ni^{II}TMpyP-4) were a gift of Dr. Pasternak. Stock solutions [$(1.4–3) \times 10^{-4}$ M] were made in 10 mM phosphate buffer, pH 7, and stored at 4 °C. Porphyrin concentrations were determined spectrophotometrically with $\epsilon_{424nm} = 2.26 \times 10^5$ L/(mol·cm) for H_2TMpyP-4 and $\epsilon_{418nm} = 1.49 \times 10^5$ L/(mol·cm) for Ni^{II}TMpyP-4. Poly(ethylene glycol) (PEG 8000) was purchased from Sigma (P.2139). All the other chemicals were reagent grade and were used without further purification.

Preparation of Liquid-Crystalline Phases of DNA. Highly polymerized calf thymus DNA (Sigma D-1601, type I) was dissolved in 10 mM Tris-HCl buffer, pH 8, at a concentration of 50 mg/mL, with overnight magnetic stirring at 4 °C. In

order to obtain short DNA fragments, the solution was sonicated at 0 °C as described previously (Livolant, 1986). DNA was precipitated in cold absolute ethanol, stored at −20 °C, pelleted, and air dried. DNA was resuspended in small volumes of 10 mM Tris-HCl, pH 8, and stored at 4 °C.

We used two methods previously described in order to obtain cholesteric liquid-crystalline phases of DNA (Livolant, 1986). They are briefly recalled here: (1) The polymer- and salt-induced cholesteric phase (PSI DNA) is produced by adding to 200 μL of 1 mg/mL sonicated DNA solution an equal volume of 400 mg/mL PEG 8000 in 2 M KCl. This mixing takes about 30 min under continuous magnetic stirring. A phase segregation occurs between DNA and PEG. The condensed DNA aggregates are deposited between quartz cover slips, and the cholesteric organization is observed at the periphery of the aggregates. (2) A drop of a highly concentrated DNA solution [25–50 mg/mL in 10 mM Tris-HCl, pH 8, 1 mM ethylenediaminetetraacetic acid (EDTA)] was deposited between quartz slides, and the preparation was allowed to concentrate. The cholesteric liquid-crystalline phase organizes progressively in some areas of the preparation.

The nature of the liquid-crystalline phases were determined by analyzing their textures in the polarizing microscope, as previously described by Livolant (1986). The helical pitch P was measured with a micrometer, in the polarizing microscope, in regions showing a perfect vertical orientation of the layers. The situation is described in detail in Figure A2 of the Appendix. The periodicity observed between crossed polarizers corresponds to half the helical pitch and can be easily measured by comparison with a micrometer plate standard under the same magnifying power.

Culture Conditions of the Dinoflagellates. A strain of the dinoflagellate *P. micans* was purchased from the Culture Collection of Algae, Department of Botany, University of Texas at Austin, Austin, TX 78713-7640. The cells were grown in the ESLP culture medium (100 cm^3 of filtered water, 50 cm^3 of soil extract, and 10 cm^3 of 2 g/L Na_2HPO_4) added with vitamins (0.6 μg/mL biotin, 1 μg/mL vitamin B-12, and 5 μg/mL thiamin) and trace metals [0.6 mL of the PIV metal solution of Starr (1978) for 100 mL of the culture medium].

The cells were cultivated in small volumes in glass flasks with a large aperture and illuminated with cool fluorescent tubes with a photoperiod of 16 h of light and 8 h of dark. The temperature was stabilized around 20 °C.

Observation of Cells in the CD Microscope. The living cells were spun at 1085g for 10 min in a Sorvall R-C2 centrifuge (SS-34 rotor), resuspended in 10 mM Tris-HCl, pH 7.4, and spun again in the same conditions. The cells were resuspended in a small volume of the same buffer added with dye.

The final concentrations of Hoechst 33342, ethidium bromide, H_2TMpyP-4, and Ni^{II}TMpyP-4 were adjusted to 50 μM in the incubation buffer. Some experiments were done in the incubation buffer added with 1 mM $CaCl_2$ and 0.35 M sucrose or in the culture medium without any difference in the results.

To obtain extruded nuclei, an aliquot of the pellet was suspended in the same buffer added with 1 mM $CaCl_2$ and 0.35 M sucrose, which was described as a good isolation medium for these nuclei (Herzog & Soyer, 1983). The cells were gently squashed between two quartz cover slips, and a drop of the same solution was immediately added to resuspend the cell components. Only the nuclei showing a regular shape were selected to do the measurements. These were assumed to be nearly in their intact state. A drop of the intact or squashed cells suspension was then mounted between two quartz cover slips sealed with silicon grease.

CD Microscopy. The CD microspectrophotometer was previously described (Maestre & Katz, 1982). It is a modification of a Cary 60 machine associated with a Zeiss UV microscope.

Without any staining, the nuclei were recognized by using the birefringence properties of these chromosomes (Livolant, 1978). To do this, the Pockels modulator was turned off to get a linearly polarized light and a Polaroid was added on the top of the ocular and rotated to reach the complete extinction. Other components of the cell are birefringent, namely, the cell wall and the starch granules, but there is no possible confusion with the nucleus.

After staining with Hoechst dye or ethidium bromide, the nuclei were easily recognized by their fluorescence at the appropriate wavelength. However, after incubation in H_2TMpyP-4 or Ni^{II}TMpyP-4 the fluorescence of the nuclei was not strong enough to be detected in the CD microscope. In these cases we used the birefringence properties of the nuclei to localize them.

The cells were positioned in the field of view of the microscope, and the nuclei were centered. A small portion of each nucleus was analyzed by inserting a pinhole between the objective lens and the photomultiplier tube. The real size of the pinholes used with the 32× and 100× objectives were respectively 0.25 and 0.63 mm, which corresponds to a real analyzed surface area of 7.8 and 6.3 μm in diameter. Considering the size of the available pinholes, it was not possible to analyze exactly the same surface area with the two objectives.

The nuclei were scanned from 500 or 370 to 240 nm. Sometimes, the intensity of the transmitted light was not strong enough at low wavelengths, and in such cases the scan was stopped when the dynode intensity reached 900 V. The position of the nucleus was checked at the end of each scan, and background scans were run by placing the pinhole of the same diameter over an empty area just near the cell.

The 32× objective (N.A. 0.4 glycerol immersion) and 100× objective (N.A. 1.25 glycerol immersion) have different half-acceptance angles: 15.5° and 56.4°, respectively. Thus, the analysis of the same area with the two objectives provided us information on the amount of light scattered in the region comprised between 15.5° and 56.4° from the forward direction (see details in Appendix, Figure A3). The effect of UV irradiation was detected by scanning the same area several times. Since it appeared to be significant (see Results), the order of the measurements with the 32× and 100× objectives was alternated to average these effects on the two series of experiments.

Signal Processing. Each scan was averaged by summing up to 2032 times for each 10-Å interval in the spectra.

Two species of data were stored for each scanned nucleus: the CD signal and the extinction signal. Each one was base line substracted and multiplied by the proper calibration factors to get the ellipticity (θ), which is related to the CD = $A_L - A_R$ by the relation $\theta = 2.303(A_L - A_R)180/4\pi$, and the extinction values $A = [(A_L + A_R)/2]$. The calibration factors were determined by scanning standard solutions in the same conditions: d-10-camphorsulfonic acid (99.98 g/L) for CD and a solution of 60 mg/mL $K_2Cr_2O_7$ in 10^{-2} M KOH for the extinction. The data were then smoothed by a third-degree 13-point interpolation routine (Tomlinson, 1968).

For the cholesteric liquid-crystalline phases of DNA the signal was too strong to be recorded in the usual way. It was necessary to use an external lock-in amplifier with a shift of

the zero to the positive values. The signal of the lock-in amplifier was then sent to the computer.

Results

In the classical CD machines following the design of Grosjean and Legrand (1960) the signal obtained by electronic means is a ratio of intensities of the difference of transmitted right and left circularly polarized light to the total intensity:

$$\text{CD signal} \approx (I_R - I_L)/(I_R + I_L)$$

where I_R and I_L are the intensities of transmitted right and left circularly polarized light respectively.

If there is only a differential absorbance, i.e., no differential scattering, then

$$\text{CD} = A_L - A_R = (2/2.303)[(I_R - I_L)/(I_R + I_L)]$$

where A_L and A_R are extinctions of left circularly polarized light and right circularly polarized light, respectively, since intensity of the transmitted light and absorbance are related by the classical formula (Beer–Lambert law)

$$I = 10^{-A} I_0$$

However, a differential scattering can be superimposed to the differential absorption. Therefore, the CD signal has to be modified and expressed as follows:

$$\text{CD} = A_L - A_R = (a_L - a_R) + (s_L - s_R)$$

$a_L - a_R$ being the intrinsic differential absorbance and $s_L - s_R$ the differential scattering cross section of the preparation.

(*1*) *Absorption Effect.* The absorption effects have been well understood in dilute solution and, according to the Beer–Lambert law

$$a_L - a_R = (\epsilon_L - \epsilon_R)cl$$

ϵ_L and ϵ_R being the molar extinction coefficients, c the concentration of the solution, and l the path length. A solution of molecules showing a right-handed helicity is known to absorb more of the left-handed circularly polarized light as in the case of DNA polymers (Tinoco, 1962). However, the CD of condensed optically active structures are of a much more complex nature. Attempts at a theoretical explanation by Keller and Bustamante (1986a) explain some of the main properties observed in Ψ-type particles, but the theory at present cannot be directly applied to the CD of such complicated organizations as the dinoflagellate nuclear structure.

(*2*) *Scattering Effects in Liquid-Crystal Organizations.* The scattering effect has been more studied. This effect is particularly important in cholesteric liquid crystals. As shown previously be de Vries (1951) and many other authors, a Bragg reflection occurs and produces a selective reflection of circularly polarized light when the helical pitch of the structure is of the same order as the wavelength of the incident light according to the relation:

$$m\lambda = P \sin \alpha$$

m being the order of the reflection, λ the wavelength of the reflected light in the medium ($\lambda_{medium} = \lambda_{vacuum}/n$, where n is the refractive index of the solution), P the helical pitch, and α the angle separating the direction of the incident light and the planes of the cholesteric layers.

The handedness of the reflected and transmitted light is directly related to the handedness of the cholesteric structure itself: for a left-handed cholesteric structure the left-handed circularly polarized light is selectively reflected whereas the right-handed circularly polarized light is transmitted, and conversely for a right-handed cholesteric structure [review in de Genes (1974)]. Generalized interaction with helical structures and twisted ladders has been considered in detail in the papers by Keller and Bustamante (1986a,b) and Kim et al. (1986).

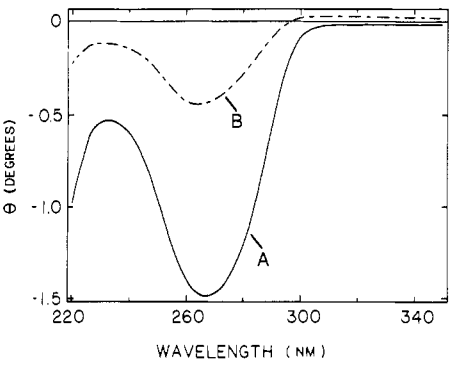

FIGURE 1: CD spectra of cholesteric phases of DNA obtained in Ψ conditions: (A) Planar cholesteric texture; (B) center of the aggregate which presents unanalyzable textures.

CD Spectra of Cholesteric Liquid-Crystalline Phases of DNA. A first series of experiments (not shown) were done with cholesteric liquid-crystalline phases of DNA obtained without addition of any polymer and proteins. Selected areas of domains with textures showing a regular periodicity of the cholesteric layers were analyzed in the CD microscope. In such regions, the cholesteric axis is lying in the preparation plane and the helical pitch (P) was measured with a micrometer. It was about 2.5 μm (2500 nm), which is very far away from the wavelength range of the machine (190–800 nm). Therefore, it was impossible to get any signal of the reflection band, but the intent was to be sure to separate completely the signals of the reflection from that of the absorption bands. A very strong negative signal was recorded in the region of the DNA absorption band. However, the preparations were optically dense, and there was not enough light to complete the scan through the absorption of the DNA at 260 nm.

A second set of experiments were done with large Ψ DNA aggregates which were less optically dense and permitted measurements down to 220 nm. The cholesteric organization appears in a few minutes at the periphery of the DNA aggregates, whereas the central parts which are highly birefringent present textures that are too small to be resolved in the optical microscope. Figure 1 shows the CD signal in the absorption band of DNA either in a perfectly defined planar texture (with the cholesteric axis parallel to the optical axis of the microscope, curve A, Figure 1) or in the central part of the aggregate (curve B, Figure 1). A very strong negative lobe is observed in both cases at 265 nm. This corresponds to a negative Ψ-type spectra but with an intensity that is several times higher than those recorded with suspensions of the usual Ψ DNA aggregates. In these planar cholesteric textures it was not possible to measure directly the helical pitch, but we suppose that is was also far away from the absorption band of DNA for two reasons: first, because in nearby regions showing another orientation of the helical axis, the helical pitch was shown to be higher than 2 μm and, second, because the shape of the CD curve is similar to those recorded in the previous set of experiments.

We can then consider that this very strong negative CD signal in the absorption band of DNA corresponds to the superorganization of the DNA molecule. The negative sign of the CD indicates that the cholesteric structure is left-handed, and this will be discussed in detail later.

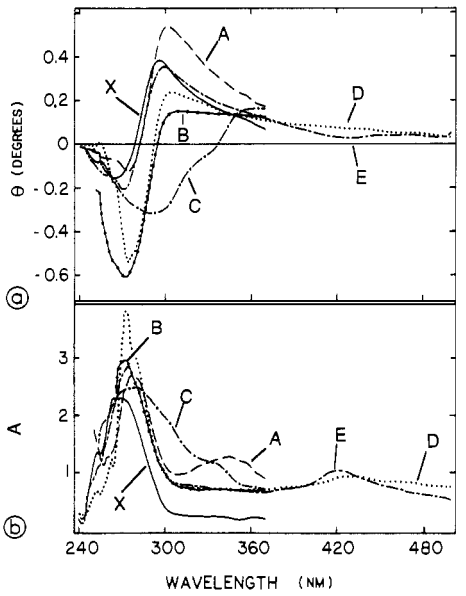

FIGURE 2: CD spectra (a) and absorption spectra (b) of birefringent *P. micans* nuclei (X) and of dyes bound to the same nuclei: Hoechst, 33342 (A), ethidium bromide low incorporation (B) and strong incorporation (C), and porphyrins H_2TMpyP-4 (D) and Ni^{II}TMpyP-4 (E).

Moreover, in the central part of the aggregate, DNA probably has also a cholesteric liquid-crystalline organization since the signal shows the same shape. However, the smaller amplitude of the signal at 265 nm supports the hypothesis that these regions correspond to a large number of small domains, each of them having a different orientation of the cholesteric axis. Such a disordered distribution of microdomains would produce textures that are nearly impossible to analyze in the optical microscope, and the averaged orientation of the helical axis with respect to the direction of the incident light will decrease the signal.

CD Analysis of Dinoflagellate Nuclei. A total of 130 individual nuclei were analyzed in the CD microscope. The spectra appeared to be highly reproducible, and we present here the average curves for each series of experiments.

Contrary to the situation described in the cholesteric liquid-crystalline phase of DNA, we are here considering a material in which the reflection and absorption bands are very close together since the helical period of the structure = 250 nm (Livolant & Bouligand, 1978) and λ_{abs} = 260 nm.

The birefringent nuclei observed inside of the living cell, without any modification of their structure, either by mechanical or chemical means, are considered here as the reference material. These nuclei present a large positive CD signal around 295 nm and a smaller negative one around 260 nm (curve X, Figure 2a).

Different dyes were inserted in the nuclei. Hoechst 33342 is known to insert obliquely in the small grove of the DNA molecule. In comparison, ethidium and porphyrins (Ni^{II}TMpyP-4 and H_2TMpyP-4) are intercalative dyes which insert parallel to the bases planes (LePecq & Paoletti, 1967; Pasternak et al., 1984). Their main absorption bands are centered away from the absorption band of DNA [λ_{abs}(porphyrin) = 420 nm, λ_{abs}(ethidium) = 285 nm, and λ_{abs}(Hoechst 33342) = 340 nm]. We were expecting to observe a mimicking signal in the absorption band of porphyrins and a reverse signal in the absorption band of Hoechst 33342 according to the results of Phillips et al. (1986). The insertion of the dyes was checked either by the induced fluorescence when it was possible (Hoechst 33342 and ethidium) or by looking at the absorption curves that were recorded simultaneously with the CD data. The average absorption curves are presented in Figure 2b. The absorption band of DNA appears to be shifted from 260 to 275 nm. Whatever the nature of the chromophores, the incorporation of dyes (curves A–E, Figure 2a) always produces a red shift of the CD spectra (comparison with the reference curve, curve X, Figure 2a).

After incubation with Hoechst 33342, we scanned only the nuclei that were fluorescent. The insertion of this dye checked in the absorption curve (curve A, Figure 2b) produces mostly an increase of the positive lobe in the CD curve (curve A, Figure 2a).

In the same way, after incubation of the cells in 50 μM ethidium only the fluorescent nuclei were analyzed. Two groups of curves were obtained, and they correspond to two different amounts of inserted dye as can be seen by looking at the two corresponding absorption curves. The group of cells showing a "small amount" of inserted dye show a very strong increase of the negative CD lobe at 265 nm and a decrease of the positive one (curve B, Figure 2a). The cells showing a strong insertion of the dye present a completely different CD curve with a strong negative CD signal between 240 and 340 nm (curve C, Figure 2a).

The effects of the insertion of porphyrins were more difficult to follow because of the lack of fluorescence: it was not possible to choose, in the population of cells, those showing a fluorescent nucleus which had obviously incorporated the dye. The average CD and absorption curves after incubation with H_2TMpyP-4 and Ni^{II}TMpyP-4 are however presented as curves D and E, respectively, in Figure 2. The two absorption curves present a general increase of the values with respect to the reference ones and a bump around 420 nm for Ni^{II}TMpyP-4. This shift is probably related to an insertion of the dyes since we observe that the average CD curves are also different from the reference one (the birefringent nuclei without any inserted dye, curve X, Figure 2). Both porphyrins produce a general red shift of the curve. Ni^{II}TMpyP-4 does not produce any other modification. A significant decrease of the positive lobe (at 300 nm) associated with a large increase of the negative one (at 270 nm) is observed with H_2TMpyP-4 (curve D, Figure 2a).

However, for the case of Ni^{II}TMpyP-4 more precise information can be extracted from the data if we consider the curves individually, because the averaging includes a lot of cells having integrated a very low amount of dye. Therefore, two curves corresponding to two different nuclei having undoubtedly incorporated two different amounts of dye are presented in Figure 3. Curve 1 corresponds to a medium incorporation (see the absorption curve, Figure 3b) and presents the reduction of the positive lobe and the increase of the negative lobe previously described with the other porphyrin (H_2TMpyP-4) (Figure 2). A stronger incorporation (curve 2) produces this effect as well, but a negative CD spectrum is also observed in the absorption band of the dye itself. We think that these two curves give a good representation of the interaction with this dye.

Effects of the Dyes. In order to present these results more clearly, the effects of the insertion of dyes are displayed in Figure 4 by subtracting the reference curve from the curves of the dinoflagellate nuclei after insertion of the dyes. The absorption curves (not shown) clearly indicate that the dyes have been incorporated in the DNA. Two effects are observed both in the absorption band of the dye and in the absorption band of DNA.

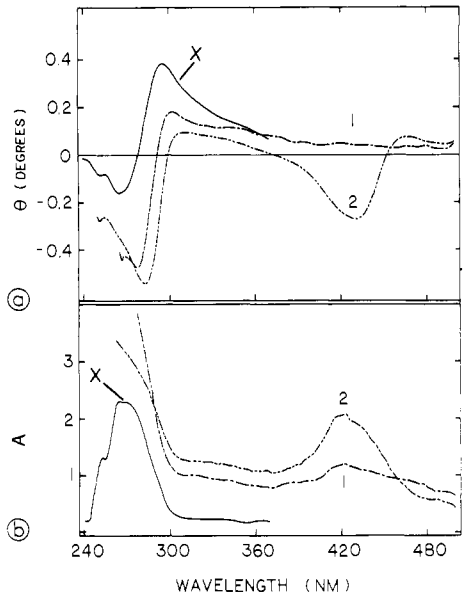

FIGURE 3: CD spectra (a) and absorption spectra (b) of a small (1) and large amount (2) of $Ni^{II}TMpyP-4$ incorporated in the dinoflagellate nucleus. The reference curve (X) corresponding to the birefringent nucleus is indicated for comparison.

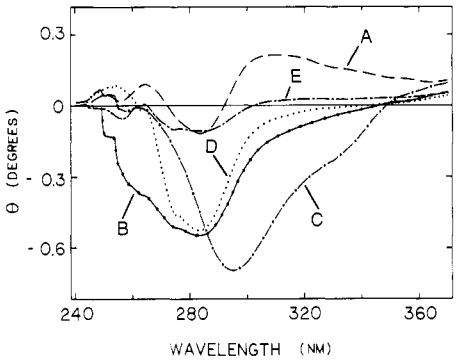

FIGURE 4: CD effects of the dyes obtained by subtraction of the reference curve from the curves presented in Figure 2: Hoechst 33342 (A), ethidium low incorporation (B), ethidium strong incorporation (C), $H_2TMpyP-4$ (D), and $Ni^{II}TMpyP-4$ (E).

(*A*) *The Dye Absorption Band.* Hoechst 33342 presents a positive CD spectrum in its absorption band (340 nm, curve A, Figure 4) whereas ethidium presents a negative CD (around 290 nm) whatever the amount of dye inserted (curves B and C, Figure 4). Similar negative CD signal is also observed in some nuclei having incorporated a significant amount of $Ni^{II}TMpyP-4$ (curve 2, Figure 3), but we do not have enough of these nuclei to get average curves of this effect. These results are in accordance with the results presented by Phillips et al. (1986). In their absorption bands, ethidium and porphyrins are mimicking the signal of the PSI-type DNA whereas Hoechst 33342 gives a reverse signal.

(*B*) *The Absorption Band of DNA.* The insertion of intercalative dyes (ethidium and porphyrins) produces a strong increase of the negative CD signal around 275 nm (curves B–E, Figure 4). This effect is very large with ethidium and $H_2TMpyP-4$. The amplitude of this effect is not so large with $Ni^{II}TMpyP-4$ perhaps due to the lack of efficient incorporation into the nuclei. We do not know if the negative CD of Hoechst 33342 around 285 nm is significant (curve A, Figure 4).

This increase of the signal could be due to an interaction effect due to a superposition of one absorption band of the dye to the absorption band of the DNA, which would have significantly increased the signal. The absorption band of ethidium (λ_{abs} = 285 nm) is not very far from the DNA absorption band (λ_{abs} = 260 nm), and the porphyrins also present a small absorption band in this region.

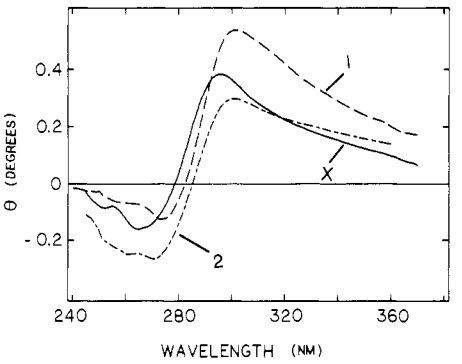

FIGURE 5: CD spectra of *P. micans* nuclei stained with Hoechst 33342 either in intact cells (1) or after extrusion out of the cells (2). The continuous line (X) corresponds to the reference curve.

Comparison of Intact and Isolated Nuclei. Two sets of data were recorded: the nuclei in the intact cell (curve 1, Figure 5) and the intact nuclei extruded out of the cells (curve 2, Figure 5). In both cases, the nuclei were recognized visually by their fluorescence after being stained in the same conditions with 50 mM Hoechst 33342. The average curves obtained for both cases are shown in Figure 5. Their shape is nearly the same, with the same amplitude, but we observe a decrease of the positive lobe and an increase of the negative one associated with a slight red shift when the nuclei are isolated.

Since we obtained a signal of the same nature, this indicates that the signals recorded in the whole cells correspond really to the nuclei and not to other cytoplasmic components. However, the difference between the intact versus extruded nuclei curves may be significant. Two explanations can be proposed: (i) The extrusion of the nuclei out of the cell could have modified the respective orientation of the chromosomes inside of the nucleus. We took all possible precautions to measure the nuclei in their intact shape (only the nuclei showing a general shape and size similar to the shape of the nucleus in the cell were analyzed), but some modifications could have occurred anyway. The more plausible modification could be a flattening of the nucleus itself and a change in the organization of the chromosomes inside of the nucleus. Indeed, a helical organization of the chromosomes was observed in decondensed nuclei (Livolant, 1984b). We do not know if the same helical organization of the chromosomes exists in the intact nucleus, but an internal order is probably present and could be modified by the squash. (ii) A possible decondensation of the chromosomes themselves could also be suggested. It has been reported that when spread on distilled water, the cholesteric structure of the dinoflagellate chromosome disappears and is replaced by a double-helical bundle of filaments (Haapala & Soyer, 1973; Livolant & Bouligand, 1980). However, in the present case, we use a solution that prevents any decondensation of the chromosomes (Herzog & Soyer, 1983), and their aspect was monitored in the microscope for signs of decondensation.

Controls. As stated previously, the similarity of a very strong signal obtained with the nuclei in the cell or after extrusion in the isolation medium indicates that the nucleus itself is responsible for the signal.

Moreover, several other control curves have been obtained. The isolated cell walls that are sometimes found in old cultures give a completely flat spectrum. We scanned also several times the cytoplasm of the intact cells outside of the fluorescent region of the nucleus with no signal measured in the same

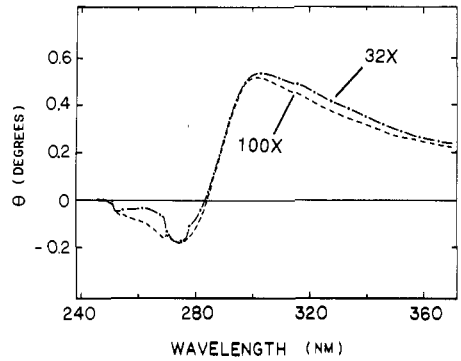

FIGURE 6: CD of seven different nuclei scanned both with the 32× objective (32×) and with the 100× objective (100×).

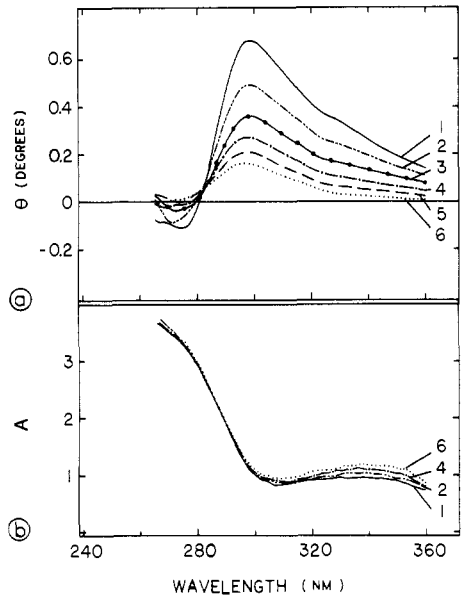

FIGURE 7: CD spectra (a) and absorption spectra (b) of the same nucleus, inside of the cell, which has been scanned six times successively. Only four absorption curves have been plotted to make the drawing clearer.

range of sensitivity (curves not shown).

CD–Circular Intensity Differential Scattering (CIDS). Seven intact nuclei stained with 50 μM Hoechst 33342 were scanned successively with the 32× and 100× objectives without any displacement of the preparation. The two average curves presented in Figure 6 indicate that there is no significant difference between them. As described under Materials and Methods and in the Appendix, the 32× and 100× objectives have half-acceptance angles of 15.5° and 56.4°, respectively. Since we got the same curve with the two objectives, this indicates that the amount of light scattered in the directions comprised between 15.5° and 56.4° from the forward direction is negligible. With the microscope it was not possible to detect the light scattered either in the side or in the back direction.

Effects of the UV Irradiation. Some nuclei were scanned consecutively a great number of times, exactly in the same conditions (100× objective). Each scan took about 17 min, which corresponds to a total UV irradiation time of more than 1 h 30 min after six scans. Both nuclei were stained with 50 μM Hoechst 33342, but one was inside of the cell (Figure 7) whereas the other one was isolated (Figure 8). In both cases we note a significant decrease of the CD signal and a simultaneous increase in the amplitude of the absorption curves. This effect is particularly important in the case of the isolated nucleus, but we must mention that other isolated nuclei (curves not shown) do not present so dramatic a modification of the

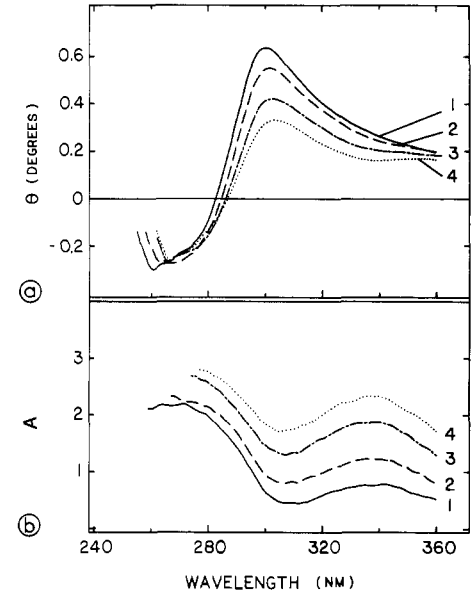

FIGURE 8: CD spectra (a) and absorption spectra (b) of another *P. micans* nucleus, extruded out of the cell, which has been scanned four times successively.

absorption but an effect similar to those observed in the nucleus inside of the cell.

Discussion

The selective reflection of one circularly polarized component of the light by cholesteric liquid crystals has been well understood many years ago by Oseen (1933) and de Vries (1951) and successfully tested experimentally with lyotropic liquid crystals (Robinson, 1961, 1966). This effect explains the anomalous apparent CD produced in their reflection band by cholesteric liquid-crystalline phases. The case of the CD observed in the absorption bands of molecules constituting the cholesteric liquid-crystalline phase or inserted in these phases (liquid crystal induced circular dichroism or LCICD) seems to be less clear. Indeed, much work has been done by introducing absorbing molecules as guest molecules in cholesteric phases and by varying the helical pitch of the structure to get different relative wavelength positions between the reflection band of the structure and the absorption band of the guest chromophore (Saeva, 1979). It appears that the sign of the LCICD (in the absorption band of the guest chromophore) depends on numerous factors: (i) the chirality of the cholesteric helix; (ii) the orientation of the transition dipole in the absorbing molecule; (iii) the preferred orientation of the molecule with respect to the long axis of the liquid-crystal molecule; (iv) the position of the wavelength of the cholesteric pitch band (λ_0) relative to the wavelength of the absorption band (λ_{abs}) (Saeva et al., 1973).

The positive or negative signs of the LCICD have been reported in a table Saeva et al. (1973) for the case of cholesteryl chloride–cholesteryl nonanoate mixtures with a transition dipole of the inserted chromophore parallel to the long axis of the liquid-crystal molecule, but we do not know whether these rules can be applied to any other situation.

DNA Cholesteric Structure. The very strong CD signal measured in the absorption band of DNA is undoubtedly related to the long-range helical organization of the structure and cannot be due to a modification of the secondary structure of the DNA molecule. Indeed, the shape of the CD signal closely resembles the Ψ-type CD spectra obtained with DNA aggregates in which the secondary structure of DNA has been shown to be unchanged, in its B form (Maniatis et al., 1974).

Moreover, this signal was expected in the absorption band of DNA as a LCICD signal since DNA is an absorbing molecule constituting a cholesteric mesophase. The amplitude of the signal, which is more than 10 times higher than the signal reported in Ψ DNA aggregates (Maestre, personal communication), reveals a much higher degree of organization and a long-range order. However, optical theories at present have not been developed enough to be able to explain in detail the interaction of light with these very dense and highly ordered structures.

The negative sign of the CD indicates that the cholesteric phase is left-handed. Maestre and Reich (1980) have shown, in films of DNA, that the sign of the CD, in the absorption band of DNA, is directly related to the sense of twist of the film. A negative CD corresponds to a left-handed twist between molecules and a positive CD corresponds to a right-handed twist. Maestre and Reich also observed two bands in the CD of their films (around 210 and 275 nm). Moreover, a strong reflection band was measured in the DNA films, indicating a cholesteric-like behavior. These results were interpreted by the authors as different modes of interaction (of higher order in m in the Bragg law) of a helix with a large repeat with respect to the wavelength of light. They supposed that their absorption and reflection bands were superimposed and that they were observing a Borrmann effect as described in Suresh (1976). The same hypothesis was also proposed in the Ψ DNA aggregates (Maestre & Reich, 1980), suggesting that the helical pitch of the helical aggregate was close to the wavelength of light at which these strong CD signals were observed.

We also observe these two bands in the planar cholesteric textures of DNA (curve A, Figure 1), measured through the CD microscope. However, in the measurements for the cholesteric DNA liquid crystals there is no evidence for a measured CD reflection band in this range of wavelengths since the helical pitch of the cholesteric phase has been estimated (around 2500 nm). The reflection band for $m = 1$ is therefore located at about 2500 nm, the higher order reflections, for $m > 1$ being forbidden for a circularly polarized light beam normal to the planes of a perfect cholesteric liquid crystal (de Gennes, 1974). On the other hand, higher order interactions probably exist inside the liquid crystal since the wave is now interacting with a dense collection of chromophores in every direction of the scattering wave (Keller & Bustamante, 1986a,b). It is probable that the very strong CD signal is a manifestation of a coupling of the near and intermediate fields with the closely packed and twisted layers of the DNA in the cholesteric liquid crystal. A possibility in favor of this hypothesis would be that we are seeing in the absorption band the effect of a higher order scattering band ($m = 7$ or 8) in the relation $m\lambda = P$.

Usually, the apparent CD is expressed as

$$\mathrm{CD} = (a_L - a_R) + (s_L - s_R)$$

$a_L - a_R$ is located at the absorption band of the chromophore whereas $s_L - s_R$ is situated at the wavelength corresponding to the helical pitch of the structure (see Appendix, section D, for detailed explanation). Therefore, these two terms can be separated if the wavelengths of the absorption band of the chromophore is far enough from the wavelength at which occurs the selective reflection of light.

The signal observed in the reflection band ($s_L - s_R$) will be positive for a left-handed structure and negative for a right-handed structure. This can be understood easily since the signal recorded in the machine is proportional to $(I_R - I_L)/(I_R + I_L)$ and helical structures of a given handedness are known

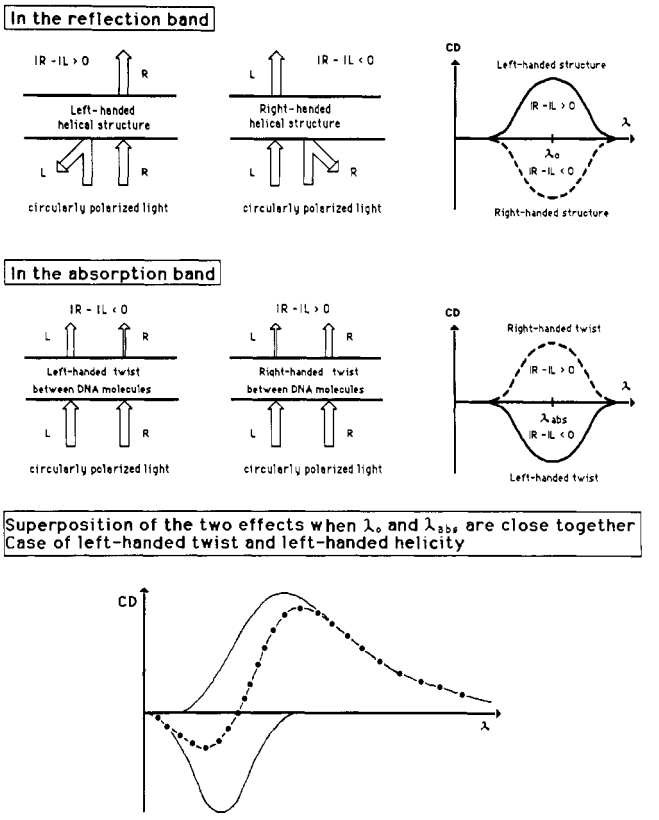

FIGURE 9: Schematic drawing summarizing the two effects that occur in CD measurements of cholesteric structures of DNA: A selective reflection of one circularly polarized component of the light occurs at a wavelength λ_0 related to the helical pitch P by the relation $\lambda_0 = nP \sin \alpha$. The difference in the transmitted intensity of right versus left circularly polarized light is positive, and the measured signal is positive. The situation is reversed for a right-handed helical structure. However, in the absorbance band of DNA (300–240 nm), a strong preferential absorption of right circularly polarized light will be measured for structures with a left-handed twist between the DNA molecules. Therefore, a left-handed helical superstructure with a left-handed twist between the DNA molecule will give a resultant positive reflection band outside of the absorbance band, i.e., $\lambda = 300$ nm for DNA, and a negative Ψ-type absorbance.

to scatter preferentially the circularly polarized light of the same handedness. Therefore, the intensity of the transmitted left circularly polarized light will be reduced for a left-handed helical structure, and $(I_R - I_L)/(I_R + I_L)$ will be positive. The situation is reversed for a right-handed helical structure. Figure 9 shows a schematic description of this effect. The complete analysis is described in detail in section D in the Appendix.

In the absorption band of the chromophore, the differential absorption of left versus right circularly polarized light can be itself decomposed into two components: the classical absorption effect given by the Beer–Lambert law for helical molecules in solution $[(\epsilon_L - \epsilon_R)cl]$ and another factor that we call $\psi_L - \psi_R$, which would correspond to a resonance phenomenon in the absorption band of the chromophores produced by the scattering occurring inside of the material.

The differential absorption can then be expressed

$$(a_L - a_R) = (\epsilon_L - \epsilon_R)cl + (\psi_L - \psi_R)$$

In this way are separated the differential absorption effects due to the secondary structure of the molecule $[(\epsilon_L - \epsilon_R)cl]$, which corresponds to the classical CD curves of the A, B, and C forms of DNA, and the signal produced by the higher order helical structure $(\psi_L - \psi_R)$.

The expression $\psi_L - \psi_R$ would correspond to a measure of the density of chromophores and of the order of the helical

structure. Therefore, in highly ordered and densely packed helical structures such as the cholesteric phases of DNA this term would be several orders of magnitude higher than $(\epsilon_L - \epsilon_R)cl$. However, the term $(\epsilon_L - \epsilon_R)cl$ becomes nonnegligible when the density of chromophores is low or the order poor. This situation is probably encountered in the bacteriophage DNA (Holzwarth et al., 1974) where the recorded signal was very low. In Figure 9 there is a description of the differential Ψ-type behavior and of how when combined with the differential scattering, a signal having the characteristics of the experimentally measured curves is obtained. A selective reflection of one circularly polarized light occurs at a wavelength λ_0 related to the helical pitch by the relation $\lambda_0 = nP \sin \alpha$. Left-handed helical structures reflect selectively left-handed circularly polarized light. Therefore, the difference in the transmitted intensity of right versus left circularly polarized light is positive, and the measured CD signal, proportional to $I_R - I_L$, is also positive. The situation is reversed for a right-handed helical structure, and a negative CD signal is recorded in this case.

A strong differential absorption of left versus right circularly polarized light occurs in the absorption band of DNA (λ_{abs} = 290–240 nm) when a twist exists between highly compacted DNA molecules (Ψ-type signal). A negative CD signal is recorded for a left-handed twist between DNA molecules and a positive CD signal for a right-handed twist (Maestre & Reich, 1980). Therefore, a left-handed helical structure with left-handed twist between the DNA molecules (as in the dinoflagellate chromosome) will produce a positive CD signal in the reflection band and a negative signal in the absorption band of the chromophore. The two effects will superimpose if the two wavelengths (λ_0 = reflection band, λ_{abs} = absorbance band) at which these two phenomena occur are close together. This is a probable explanation for the CD spectra obtained from the dinoflagellates.

The Dinoflagellate Nucleus. In the dinoflagellate nuclei, the CD signal is always negative around 265 nm which can be interpreted as a left-handed helicity of DNA, by comparison with the twisted films data (Maestre & Reich, 1980). This result corroborates the determination of the sense of the helicity found by goniometric method with thin sections of these chromosomes in the electron microscope (Livolant et al., 1978; Livolant & Bouligand, 1978).

We also observed a positive CD lobe around 310 nm in a region where no component of the nucleus is expected to absorb. The absorption curves indicate that the absorbance is negligible in this region. Different hypotheses can be proposed to explain this effect, which was not observed in the cholesteric phases of DNA:

(i) An anomalous transmission effect occurs, analogous to the Borrmann effect described in cholesteric liquid crystals when the reflection and absorption bands overlapping. According to the Bragg relation:

$$m\lambda_{0,\text{medium}} = P \sin \alpha$$

We can estimate the wavelength at which occurs the selective reflection of circularly polarized light in these nuclei, taking into account that $\lambda_{0,\text{medium}} = \lambda_{0,\text{vacuum}}/n$. m is the order of the reflection, λ the wavelength of light, α the angle separating the incident light from the cholesteric planes, and n the refractive index of the medium. Then

$$m\lambda_{0,\text{vacuum}} = nP \sin \alpha$$

If we suppose that the chromosomes present all the possible orientations in the nucleus, α will vary from 0° to 90° and sin α from 0 to 1 with an average value of 0.63. If the average index of refraction of the medium is supposed to be equal to 1.5, then $\lambda_{0,\text{vacuum}}$ = 236 nm since P = 250 nm (Livolant & Bouligand, 1980). But we know that the chromosomes are not completely disordered in the nucleus but that they follow certain preferential orientations. Therefore, the angle α is probably not exactly averaged and can reach a maximum value of 90°, which gives a maximum $\lambda_{0,\text{vacuum}}$ = 375 nm. We can see that the estimation of α is particularly critical in this analysis since 236 and 375 nm are below and above the absorption band of DNA (at 260 nm) and the positive lobe (at 310 nm).

If we make the hypothesis that λ_0 and λ_{abs} are superimposed, we can apply the theory developed by Holzwarth and Holzwarth (1973). They explained this reversal of sign of the LCICD by extending the de Vries theory to the absorbing case. They added a frequency-dependent complex distribution of the spiraling dielectric tensor of the liquid crystal and observed that the CD curves fall into two classes, those having a more or less Gaussian shape for $\lambda_0/\lambda_{abs} < 1$ or > 1 and the other biphasic with a peak and trough at $\lambda_0/\lambda_{abs} = 1$. This anomalous optical effect observed when absorption and reflection bands are superimposed has been predicted and confirmed experimentally in liquid crystals (Suresh, 1976). It has been interpreted as a Borrmann effect, which originally corresponds to an anomalous increase in the transmitted X-ray intensity when a crystal is set for a Bragg reflection (Borrmann, 1941).

For a left-handed cholesteric structure, the Borrmann effect produces a decrease of the negative signal and the creation of a positive CD lobe at the lower wavelengths. This is due to an anomalous transmission of left circularly polarized light which is enhanced at the lower wavelengths side and attenuated at the higher wavelength side of the reflection band. This modification of the curve is proportional to the amount of absorbing substances. Since we have a very large amount of absorbing material (DNA), the positive lobe could then be a consequence of the anomalous transmission of the light in this wavelength range. But in a left-handed cholesteric structure, the creation of the positive lobe is expected to occur at the lower wavelengths. In our experimental results, the positive lobe is observed at the higher wavelength side.

(ii) In the dinoflagellate chromatin, DNA is associated with RNA and proteins and these components could introduce specific signals. However, proteins and RNA are not expected to produce any differential absorption effects at wavelengths that are so far from their intrinsic absorption bands. The only possibility would be the existence of a differential scattering effect. In this case, the positive sign of the CD spectra is also consistent with a left-handed helicity of the structure: since a left-handed structure scatters more the left-handed circularly polarized component of the light, the CD signal related to $(I_R - I_L)/(I_R + I_L)$ will be positive. This effect has been well understood in the case of the octopus sperm heads (Maestre et al., 1982). See Appendix, section D, for theoretical justification of the influence of differential scattering on CD signal.

Therefore, what we observe here is probably the superposition of a negative CD signal in the absorption band of DNA at 265 nm and a positive CD signal in the reflection band of the structure around 250 nm. This scattering effect probably reduces significantly the amplitude of the negative lobe at 265 nm, but the tail of the scattering lobe which extends toward the red is observed at 310 nm. These apparently opposite effects of differential absorption versus differential scattering are summarized in a schematic drawing in Figure 9.

Denaturation by the UV Irradiation. The simultaneous decrease of the CD signal and increase of the absorbance are

undoubtedly due to a denaturation of the DNA molecule by the UV irradiation. Indeed, the hyperchromicity effect is well-known to occur in DNA when the bonds between the bases are broken by either heat or UV. This effect, which has been interpreted many years ago by DeVoe and Tinoco (1962), is an additional argument showing that the reported signal is due to the DNA and not to the proteins that are present in the structure. However, we must mention that this effect is observed not only at 260 nm (the absorption band of DNA) but also between 260 and 360 nm. This probably indicates that the positive lobe at 310 nm is also due to the superstructure of DNA since the denaturation of the molecule reduces significantly the CD signal in this region. The hypothesis of a protein effect in this region can then be ruled out.

Effects of the Dyes. It appears that the intercalactive dyes (ethidium and porphyrins) which are shown to mimic the Ψ-type spectra of Ψ DNA in their absorption band (Phillips et al., 1986) also mimic the CD signal of DNA in a biological structure in vivo. Moreover, we observe that they produce a significant increase of the negative CD signal at 265 nm (in the absorption band of DNA). This effect could be explained by the existence of an absorption band of these dyes in this region (a small absorption band of porphyrins is located at 260 nm, and the absorption band of ethidium at 285 nm is not far from there). However, the amplitude of the effect cannot be explained only by this process. An interaction of these dyes with the base planes, whose nature remains to be elucidated, is probably responsible for this increase in CD signal.

Left-Handed Helicity of DNA Superorganization in Vitro and in Vivo. Many authors postulated that the sign of the Ψ-type CD spectra observed in condensed aggregates of DNA was related to the handedness of the helical twist occurring between DNA molecules, but the decisive experiment was realized by Maestre and Reich (1980) with twisted films of DNA: Ψ^- CD spectra correspond to a left-handed twist between DNA molecules and Ψ^+ CD spectra to a right-handed twist. By extension, it can be supposed that all Ψ CD spectra correspond to a left-handed twist whereas Ψ^+ CD spectra correspond to a right-handed twist, as it was later postulated by Huey and Mohr (1981).

However, if Ψ^- and Ψ^+ have both been observed, it seems that the left-handed twist is much more frequently observed in vitro as well as in vivo. This probably reveals an optimal energetic situation probably related to the shape of the molecule and to its ionic environment. The evidence for this conjecture is the following:

(i) In microaggregates of DNA the CD signal is most often negative, namely, when the condensation is induced by poly(ethylene glycol), H1 and H5 histones, polylysine, and ethanol. Some Ψ^+ spectra were however obtained for certain concentrations of ethanol and salts (Huey & Mohr, 1981) and when the condensation of DNA is produced by certain polypeptides. In this case, Shin and Eichhorn (1984) showed that the sign of the induced CD signal was dependent on the nature of the DNA and of the added polypeptides.

(ii) In this work the cholesteric phases of DNA have been shown to present a left-handed twist whatever the method of preparation of the phase, by segregation of the condensed DNA phase either in the presence of another polymer (PEG) or simply in highly concentration without anything added. Maestre and Reich (1980) also observed that DNA films spontaneously tend to give negative Ψ-type spectra.

(iii) Dubochet and Noll (1978) obtained a crystallization of nucleosome cores isolated from calf thymus chromatin. One of the crystalline forms corresponds to cylinders composed of concentric cylindrical layers of intertwined right-handed helices of nucleosome cores, and the twist occurring between DNA molecules of adjacent nucleosomes is left-handed.

(iv) Negative Ψ-type spectra were also obtained with T2, T4, and T6 bacteriophage DNA (Holzwarth et al., 1984). However, in this case, the amplitude of the signal was very small and therefore not so reliable.

(v) In the same way, the chromatin extruded from the stallion sperm nuclei has also been shown to present a very strong negative spectrum indicating the presence of a long-range left-handed cholesteric packing of DNA (Sipski & Wagner, 1977).

(vi) In biological structures, the handedness of the twist occurring between DNA molecules has also been determined in some cases, namely, in some chromosomes showing a cholesteric organization. The handedness was determined by tilting longitudinal sections of chromosomes with a goniometric stage in the electron microscope. Longitudinal sections, which are parallel to the cholesteric axis of the structure, present a periodic pattern with an alternation of lines and points, and the periodicity corresponds to the half-helical pitch. The tilt of such longitudinal sections makes series of nested arcs to appear, and the sense of the concavity of the arcs obtained for a given inclination of the preparation can be related to the handedness of the cholesteric structure. Chromosomes of two species of dinoflagellates (*Xanthella* and *P. micans*) present a left-handed twist (Bouligand et al., 1968; Livolant et al., 1978) as well as the bacterial nucleoids (Gourret, 1981).

DNA molecules are right-handed helices that are shown to produce spontaneously a left-handed twist between them when aggregated or condensed into films. An interesting model was proposed by Rudall (1955) to explain how a dense packing of helical molecules can produce a helical structure of the opposite handedness. In concentrated solutions, elongated molecules tend to align in parallel in a given plane. For minimum space requirement reasons, they tend to shift longitudinally by a quarter-helical pitch the one with respect to each other. In this way, oblique striae are created in which molecules of the next plane can align. By this process, a right-handed helical molecule will produce a left-handed twist and conversely. This theory has been shown to be helpful in the understanding of cholesteric liquid crystals which are generally constituted of helical molecules. However, a molecule of a given helicity like poly-γ-benzyl-L-glutamate (PBLG) can produce cholesteric phases of opposite handedness depending on the nature of the solvent. Therefore, it was postulated (Samulski & Tobolsky, 1974) that the ionic environment of the molecule was more important than the structural shape of the molecule itself.

In conclusion, we have shown the following:

(1) Cholesteric liquid-crystalline phases of DNA present a very strong negative Ψ-type CD signal in the absorption band of DNA (265 nm) whose very large amplitude is independent of the helical periodicity of the structure. It corresponds only to a differential absorption effect.

(2) In the dinoflagellate nucleus there is a superposition of a differential absorption effect producing a negative Ψ-type spectra around 265 nm and a differential scattering effect producing a positive lobe at 310 nm. The negative sign of the absorption lobe and the positive sign of the scattering lobe are both consistent with a left-handed helical structure of the chromatin.

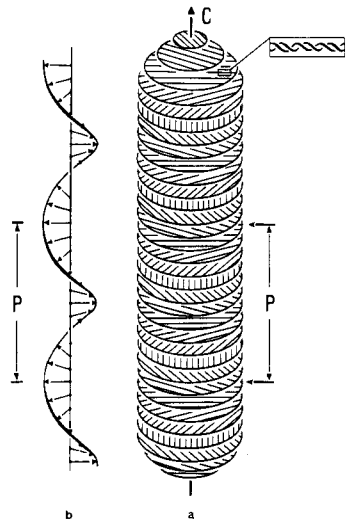

FIGURE A1: Schematic drawing of the cholesteric structure of a dinoflagellate chromosome. The helical pitch corresponds to a rotation of 360° of the molecular orientation of each DNA segment.

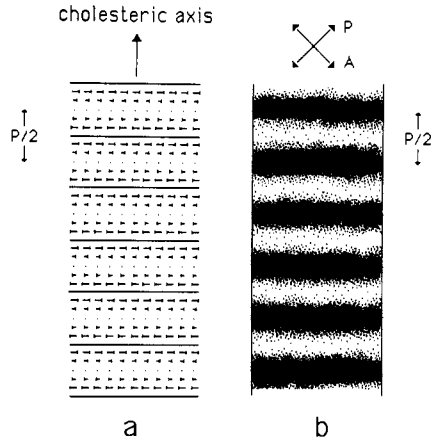

FIGURE A2: Determination of the cholesteric periodicity of liquid-crystal phase of DNA.

(3) Intercalative dyes (ethidium and porphyrins) mimic the differential absorption effect of the long-range order structure producing a negative CD signal in their absorption band. Moreover, an interaction occurs between these dyes and the base planes which increases significantly the negative signal of DNA at 265 nm.

(4) Cholesteric phases of DNA and dinoflagellate chromatin present a left-handed helical organization, and we show that this handedness seems to be the rule in most cases in vivo and in vitro. This indicates that a left-handed twist is produced spontaneously between DNA molecules, probably because of minimum-energy configurations.

(5) The apparent CD can be expressed as the sum of three components:

$$CD = [(\epsilon_L - \epsilon_R)cl] + (\psi_L - \psi_R) + (s_L - s_R)$$

The first term $[(\epsilon_L - \epsilon_R)cl]$ corresponds to a secondary structure absorption effect and is observed in the absorption band of the chromophore. The third term $(s_L - s_R)$ corresponds to a true differential scattering effect, and it can be observed at the wavelength corresponding to the helical pitch of the structure. The second term $(\psi_L - \psi_R)$ observed in the absorption band of the chromophore corresponds to an anomalous absorption effect produced by a scattering of light inside of the structure. This term is the one that gives information about the perfection of the helical order and the density of chromophores.

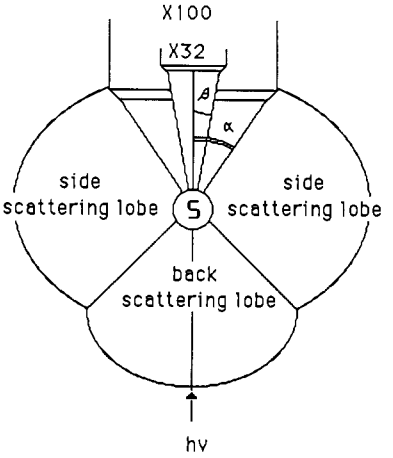

FIGURE A3: Drawing describing the spatial relationships of the scattering lobes of a particle with respect to the acceptance angles of the 32× power and 100× power objectives of the microscope.

ACKNOWLEDGMENTS

We gratefully acknowledge Dr. W. Mickols for demonstrating the use of the CD microscope and of the computer programs, and we thank Dr. R. F. Pasternak for his generous gift of the porphyrins.

APPENDIX

In this Appendix we discuss in some detail the theoretical rationale for the interpretation of the experimental data.

(*A*) *Model of Dinoflagellate Chromosome.* In Figure A1 we show a schematic representation of the cholesteric structure of the dinoflagellate chromosome. The DNA molecule is everywhere normal to the elongation axis of the chromosome, but its orientation rotates continuously, always in the same direction. This organization can be understood easily if the average orientation of the DNA molecules are indicated by fictive, parallel, and equidistant planes that are normal to the cholesteric axis (C). The helical pitch *P* corresponds to a rotation of 360° of the molecular orientations (a). We drew here a left-handed cholesteric structure. This is more easily followed if an arbitrary direction is assigned to a given molecular orientation in a plane and followed from plane to plane (b). The extremity of arrow tip draws a left-handed helix.

(*B*) *Determination of DNA Cholesteric Pitch.* The determination of the helical pitch *P* in cholesteric liquid-crystalline phases of DNA was as follows: In a cholesteric structure, the orientation of molecules rotates continuously along the direction normal to the planes of the molecules. This direction is called the cholesteric axis. When this axis lies in the observation plane, molecules are alternatively parallel, oblique, and perpendicular to this plane, and their orientation can be indicted respectively by lines, nails, and points as in (a), Figure A2. When this structure is observed in the polarizing microscope, with the cholesteric axis at 45° from the polarizer directions (P, A), the intensity of the transmitted light depends on the orientation of the molecules with the maximum when the molecules are lying in the preparation plane (lines) and a minimum when molecules are parallel to the optical axis of the microscope (points, Figure A2, panel b). Patterns with a regular alternation of dark and light stripes are then observed; the distance separating two bright or two dark lines corresponds to half the helical pitch $P/2$. This periodicity can be easily measured in the microscope.

(*C*) *Differential Scattering as a Function of Scattering Angle.* The reason we claim that the differential scattering for the *P. micans* is in the directions perpendicular to the path

of the illuminating ray or in the backward direction is because of the experimental results of Reich et al. (1980). In Figure 3 of that paper there is scattering measurement on PSI-type DNA condensates as a function of acceptance angle. It can be shown in the graph that the CD spectra do not change when the acceptance angle of the photomultiplier is changed from 14° acceptance to about 113° of acceptance. However, when the acceptance angle is increased to 247° by the use of fluorscat cuvettes, the scattering contribution to the CD curve disappears, which implies that the differential scattering in the region from 113° to 247° is recovered.

In the CD microscope it is not possible to measure the scattering effect of a sample (object S in Figure A3) in the side or back directions. We can only detect the amount of light scattered in the cone comprised between α and β (Figure A3) from the forward direction by using the 32× and 100× power objectives having two different acceptance angles: $\alpha = 56.5°$ and $\beta = 15.5°$.

(D) Sign of Differential Scattering as a Function of Sense of Helix. Concerning the interpretation of the positive differential scattering contribution of the nucleus, the theory shows that this is due to a left-handed helix as follows: This differential scattering band occurs outside the major absorbance bands of the nuclei. Accordingly, it is described by the equation (Bustamante et al., 1983):

$$\mathrm{CD} = \left(\frac{2}{2.303}\right)\frac{I_R - I_L}{I_R + I_L} = (a_L - a_R) + (s_L - s_R) + \frac{\sigma_L(0) - \sigma_R(0)}{2r^2 + \sigma_L(0) + \sigma_R(0)} \quad \text{(A1)}$$

where R and L are symbols for right and left circularly polarized light. The circular differential scattering cross section is the important part in this equation in the regions of the spectrum where there is no absorbance. This term is

$$\mathrm{CD}(\theta) = [s_L(\theta) - s_R(\theta)] + \frac{\sigma_L(0) - \sigma_R(0)}{2r^2 + \sigma_L(0) + \sigma_R(0)} \quad \text{(A2)}$$

where

$$[s_L(\theta) - s_R(\theta)] = \frac{N_0}{2303}\int_0^{2\pi} d\phi \int_0^{\theta} [\sigma_L(\theta') - \sigma_R(\theta')] \sin\theta' \, d\theta' \quad \text{(A3)}$$

and the scattering cross section for right or left circularly polarized light is

$$\sigma_{R,L}(\theta') = r^2 \frac{I_{R,L} \cos\theta'}{I_{R,L,0}} \quad \text{(A4)}$$

The second term in eq A2 represents the contribution from the light scattered forward along the incident beam (i.e., $\theta = 0$). This contribution depends on the effective optical distance r from the lens center. The second term is the same for the 32× power objective and for the 100× power objective. Consequently, by subtraction of the 32× power objective spectra from the 100× power objective spectra, that term is effectively canceled. The first term depends on the angle of capture of the different objectives, $\theta_1 = \alpha$ and $\theta_2 = \beta$ in Figure A3. If the substracted spectra show the same scattering behavior (outside the absorbance bands of the nuclei), this implies that the forward scattering, in the region of the scattering envelope defined by the difference in acceptance angles of the objectives, contributes little to the differential scattering behavior to the object.

It is important to understand that a *right-handed helix* with periodicities in the range of the wavelength of the circularly polarized light would give a *negative* signal, that is, $s_L - s_R \leq 0$. This is because the scattering cross section of a right-handed helix is larger for a right circularly polarized wave than for a left circularly polarized wave. Thus, according to the equation above, $s_R \geq s_L$ and the measured CD would be negative. However, the measured CD is positive, $s_L \geq s_R$, implying that the scattering structure must be a left-helical organization. This analysis shows that the interpretation of the differential scattering component is consistent with the results of the dye measurements.

To prove further our interpretation, consider the case of a cholesteric liquid crystal with a right-handed helical structure. It is well-known for this case that when the pitch of the helix matches the wavelength of a right circularly polarized light beam, total reflection occurs of that polarization and total transmission occurs for the opposite polarization, in this case left circularly polarized light. What does this mean in terms of the CD measurement? For the transmitted beam the intensity I_R is zero because of total reflection backward whereas the left circularly polarized intensity is transmitted totally. This gives a value

$$\mathrm{CD} = \left(\frac{2}{2.303}\right)\frac{I_R - I_L}{I_R + I_L} = \frac{0 - I_L}{0 + I_L} = -1 \quad \text{(A5)}$$

i.e., a *negative signal* for the CD of a right-handed helix. For a left-handed cholesteric liquid crystal the CD signal in the reflection band would be a *positive signal.*

References

Adler, A. J., & Fasman, G. D. (1971) *J. Phys. Chem. 75*, 1516.

Babillot, C. (1970) *J. Microsc. (Paris) 9*, 485.

Borrmann, G. (1941) *Phys. Z. 42*, 157.

Bouligand, Y., Soyer, M. O., & Puiseux-Dao, S. (1968) *Chromosoma 24*, 251.

Brugerolle, G., & Mignot, J. P. (1979) *Biol. Cell. (1977–1980) 35*, 111.

Brunner, W. C., & Maestre, M. F. (1974) *Biopolymers 13*, 345.

Burchardt, G., Zimmer, C., & Luck, G. (1973) *FEBS Lett. 30*, 35.

Bustamante, C., Tinoco, I., Jr., & Maestre, M. F. (1983) *Proc. Natl. Acad. Sci. U.S.A. 80*, 3568.

Bustamante, C., Maestre, M. F., & Keller, D. (1985) *Biopolymers 24*, 1595.

de Gennes, P. G. (1974) *The Physics of Liquid Crystals*, Clarendon Press, Oxford.

DeVoe, H., & Tinoco, I., Jr. (1962) *J. Mol. Biol. 4*, 518.

de Vries, H. (1951) *Acta Crystallogr. 4*, 219.

Dubochet, J., & Noll, M. (1978) *Science (Washington, D.C.) 202*, 280.

Evdokimov, Y. M., Pyatigorskaya, T. L., Polystev, D. F., Akimenko, N. M., Kadykov, V. A., Tsvankin, D. Y., & Varskavsky, Y. M. (1976) *Nucleic Acids Res. 3*, 2353.

Evdokimov, Y. M., Salyanov, V., & Palumbo, M. (1985) *Mol. Cryst. Liq. Cryst. 131*, 285.

Gourret, J. P. (1978) *Biol. Cell. (1977–1980) 32*, 299.

Gourret, J. P. (1981) *Actual. Bot. (Bull. Soc. Bot. Fr.) 128*, 55.

Grosjean, M. J., & Legrand, M. (1960) *C. R. Hebd. Seances Acad. Sci. 251*, 2150.

Haapala, O. K., & Soyer, M. O. (1973) *Nature (London), New Biol. 244*, 195.

Haynes, M., Garrett, R. A., & Gratzer, W. B. (1970) *Biochemistry 9*, 4410.

Herzog, M., & Soyer, M. O. (1981) *Eur. J. Cell Biol. 23*, 295.
Herzog, M., & Soyer, M. O. (1983) *Eur. J. Cell Biol. 30*, 33.
Herzog, M., Soyer, M. O., & Daney de Marcillac, G. (1982) *Eur. J. Cell Biol. 27*, 151.
Holzwarth, G., & Holzwarth, N. A. W. (1973) *J. Opt. Soc. Am. 63*, 324.
Holzwarth, G., Gordon, D. G., McGinnes, J. E., Dorman, B. P., & Maestre, M. F. (1974) *Biochemistry 13*, 126.
Huey, R., & Mohr, S. C. (1981) *Biopolymers 20*, 2533.
Jordan, C. F., Lerman, L. S., & Venable, J. H. (1972) *Nature (London), New Biol. 236*, 67.
Keller, D., & Bustamante, C. (1986a) *J. Chem. Phys. 84*, 2961.
Keller, D., & Bustamante, C. (1986b) *J. Chem. Phys. 84*, 2972.
Keller, D., Bustamante, C., Maestre, M. F., & Tinoco, I., Jr. (1985) *Biopolymers 24*, 783.
Kim, M. H., Ulibarri, L., Keller, D., Maestre, M. F., & Bustamante, C. (1986) *J. Chem. Phys. 84*, 2981.
Laemmli, U. K. (1975) *Proc. Natl., Acad. Sci. U.S.A. 72*, 4288.
Lerman, L. S. (1971) *Proc. Natl. Acad. Sci. U.S.A. 68*, 1886.
Lerman, L. S. (1973) *Cold Spring Harbor Symp. Quant. Biol. 38*, 59.
Livolant, F. (1984a) *Eur. J. Cell. Biol. 33*, 300.
Livolant, F. (1984b) Thèse de Doctorat d'Etat, Université Pierre et Marie Curie, Paris.
Livolant, F. (1986) *J. Phys. (Les Ulis, Fr.) 47*, 1605.
Livolant, F. (1987) *J. Phys. (Les Ulis, Fr.) 48*, 1051.
Livolant, F., & Bouligand, Y. (1978) *Chromosoma 68*, 21.
Livolant, F., & Bouligand, Y. (1980) *Chromosoma 80*, 97.
Livolant, F., & Bouligand, Y. (1986) *J. Phys. (Les Ulis, Fr.) 47*, 1813.
Livolant, F., Giraud, M. M., & Bouligand, Y. (1978) *Biol. Cell. (1977–1980) 31*, 159.
Maestre, M. F., & Reich, C. (1980) *Biochemistry 19*, 5214.
Maestre, M. F., & Katz, J. E. (1982) *Biopolymers 21*, 1899.
Maestre, M. F., Bustamante, C., Hayes, T. L., Subirana, J. A., & Tinoco, I., Jr. (1982) *Nature (London) 298*, 773.
Maestre, M. F., Salzman, G. C., Tobey, R. A., & Bustamante, C. (1985) *Biochemistry 24*, 5152.
Maniatis, T., Venable, J. H., & Lerman, L. S. (1974) *J. Mol. Biol. 84*, 37.
Matthys, E., & Puiseux-Dao, S. (1968) *C. R. Seances Acad. Sci., Ser. D 267*, 2123.
Mickols, W., Maestre, M. F., & Tinoco, I., Jr. (1987) *Nature (London) 328*, 452–454.
Nitayananda, R., Kini, U. D., Chandrasekhar, S., & Suresh, K. A. (1973) Proceedings of the International Liquid Crystal Conference, Bangalore, Dec 1973, Suppl. I, p 325.
Oseen, C. W. (1933) *Trans. Faraday Soc. 29*, 883.
Pasternack, R. F., Antebi, A., Ehrlich, B., Sidney, D., Gibbs, E. J., Bassner, S. L., & Depoy, L. M. (1984) *J. Mol. Catal. 23*, 235.
Phillips, C. L., Mickols, W. E., Maestre, M. F., & Tinoco, I., Jr. (1986) *Biochemistry 25*, 7803.
Rae, P. M. M. (1973) *Proc. Natl. Acad. Sci. U.S.A. 70*, 1141.
Rae, P. M. M., & Steele, R. E. (1978) *BioSystems 10*, 37.
Reich, C., Maestre, M. F., Edmonson, S., & Gray, D. M. (1980) *Biochemistry 19*, 5208.
Rill, R. L. (1986) *Proc. Natl. Acad. Sci. U.S.A. 83*, 342.
Rizzo, P. J., & Burghardt, R. C. (1980) *Chromosoma 76*, 91.
Rizzo, P. J., Jones, M., & Ray, S. M. (1982) *J. Protozool. 29*, 217.
Robinson, C. (1961) *Tetrahedron 13*, 219.
Robinson, C. (1966) *Mol. Cryst. 1*, 467.
Rudall, K. M. (1955) *Lect. Sci. Basis Med. 5*, 217.
Saeva, F. D. (1979) in *Liquid Crystals, The Fourth State of Matter* (Saeva, F. D., Ed.) pp 249–273, Marcel Dekker, New York.
Saeva, F. D., Sharpe, P. E., & Olin, G. R. (1973) *J. Am. Chem. Soc. 95*, 7656.
Samulski, E. T., & Tobolsky, A. V. (1974) in *Liquid Crystals and Plastic Crystals* (Gray, G. W., & Winsor, P. A., Eds.) Vol. 1, p 175, Horwood, Chichester.
Shin, Y. A., & Eichhorn, G. L. (1977) *Biopolymers 16*, 225.
Shin, Y. A., & Eichhorn, G. L. (1984) *Biopolymers 23*, 325.
Simpson, R. T., & Sober, H. A. (1970) *Biochemistry 9*, 3103.
Sipski, M. L., & Wagner, T. E. (1977) *Biol. Reprod. 16*, 428.
Soyer, M. O., & Haapala, O. K. (1974) *Chromosoma 47*, 179.
Sponar, J., & Fric, I. (1972) *Biopolymers 11*, 2317.
Starr, R. C. (1978) *J. Phycol. 14 (Suppl.)*, 47.
Suresh, K. A. (1976) *Mol. Cryst. Liq. Cryst. 35*, 267.
Tinoco, I., Jr. (1962) *Adv. Chem. Phys. 4*, 113.
Tomlinson, B. L. (1968) Ph.D. Thesis, University of California, Berkeley, CA.
Tunis-Schneider, M. J. B., & Maestre, M. F. (1970) *J. Mol. Biol. 52*, 521.
Wolf, B., Berman, S., & Hanlon, S. (1977) *Biochemistry 16*, 3655.